Novel 2-oxoindoline-based hydroxamic acids: Synthesis, cytotoxicity and inhibition of histone deacetylation

Tran Thi Lan Huong, Do Thi Mai Dung, Phan Thi Phuong Dung, Phung Thanh Huong, Tran Khac Vu, Hyunggu Hahn, Byung Woo Han, Jisung Kim, Minji Pyo, Sang-Bae Han, Nguyen-Hai Nam

PII: S0040-4039(15)30188-X
DOI: http://dx.doi.org/10.1016/j.tetlet.2015.09.147
Reference: TETL 46819

To appear in: *Tetrahedron Letters*

Received Date: 22 January 2015
Revised Date: 18 August 2015
Accepted Date: 29 September 2015

Please cite this article as: Huong, T.T.L., Dung, D.T.M., Dung, P.T.P., Huong, P.T., Vu, T.K., Hahn, H., Han, B.W., Kim, J., Pyo, M., Han, S-B., Nam, N-H., Novel 2-oxoindoline-based hydroxamic acids: Synthesis, cytotoxicity and inhibition of histone deacetylation, *Tetrahedron Letters* (2015), doi: http://dx.doi.org/10.1016/j.tetlet.2015.09.147

Graphical Abstract

To create your abstract, type over the instructions in the template box below.
Fonts or abstract dimensions should not be changed or altered.

Leave this area blank for abstract info.

Novel 2-oxoindoline-based hydroxamic acids: synthesis, cytotoxicity and inhibition of histone deacetylation

Tran Thi Lan Huong,[a] Do Thi Mai Dung,[a] Phan Thi Phuong Dung,[*a] Phung Thanh Huong,[a] Tran Khac Vu,[b] Hyunggu Hahn,[c] Byung Woo Han,[c] Jisung Kim,[d] Minji Pyo,[d] Sang-Bae Han,[*d] Nguyen-Hai Nam[*a]

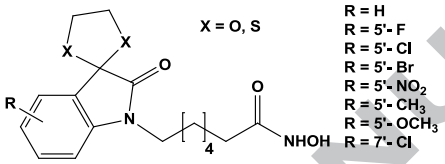

Tetrahedron Letters
journal homepage: www.elsevier.com

Novel 2-oxoindoline-based hydroxamic acids: synthesis, cytotoxicity and inhibition of histone deacetylation

Tran Thi Lan Huong,[a] Do Thi Mai Dung,[a] Phan Thi Phuong Dung,[*a] Phung Thanh Huong,[a] Tran Khac Vu,[b] Hyunggu Hahn,[c] Byung Woo Han,[c] Jisung Kim,[d] Minji Pyo,[d] Sang-Bae Han,[*d] Nguyen-Hai Nam[*a]

[a]*Hanoi University of Pharmacy, 13-15 Le Thanh Tong, Hanoi, Vietnam*
[b]*School of Chemical Engineering, Hanoi University of Science and Technology, N0 1 Dai Co Viet, Hai Ba Trung, Hanoi, Vietnam*
[c]*Research Institute of Pharmaceutical Sciences, College of Pharmacy, Seoul National University, Seoul 151-742, Korea*
[d]*College of Pharmacy, Chungbuk National University, Cheongju, Chungbuk 361-763, Korea*

ARTICLE INFO

Article history:
Received
Received in revised form
Accepted
Available online

Keywords:
Histone deacetylase (HDAC) inhibitors
Hydroxamic acids
Isatin
Heterocycle

ABSTRACT

In a continuation of a research program to discover novel small molecules targeting histone deacetylases, a series of 2´-oxospiro[1,3]dioxolane/dithiolane-2,3´-indoline-based hydroxamic acids have been designed and synthesized. These 2-oxoindoline-based hydroxamic acids displayed potent cytotoxicity against three human cancer cell lines, including SW620 (colon cancer), PC-3 (prostate cancer) and AsPC-1 (pancreatic cancer), with IC_{50} values as low as 0.05-0.07μM, 74-fold lower than that of SAHA (1.64-3.70 μM). Additionally, compounds in this series exhibited good inhibition against histone-H3 and histone-H4 deacetylation, as evaluated by Western Blot assay. These compounds also strongly inhibited HDAC2 with IC_{50} values as low as 0.03 μM. Docking studies performed using Autodock Vina showed all compounds bound to HDAC2 with relatively higher affinities (from -7.7 to -8.0 kcal/mol) compared to SAHA (-7.4 kcal/mol).

Target-based drug design and discovery has become mainstream in anticancer drug discovery and development. With the advances of the molecular biology, many molecular targets for anticancer drugs have been identified.[1] Among these, histone deacetylases (HDACs) are a group of targets which currently attract a great deal of interest from medicinal chemists worldwide.[2,3]

HDACs are enzymes that catalyze the removal of acetyl groups from specific lysine residues in the histone tails. This removal results in chromatin condensation and transcriptional repression.[2,3] Besides their involvement in the regulation of gene expression and chromatin structure, HDACs have also been demonstrated to play an important role in cell-cycle progression and carcinogenic process.[2,3] To date, 18 mammalian HDAC enzymes have been identified. These HDACs are categorized into four classes based on their structural and functional characteristics.[4] Class I containing four members include HDAC 1, 2, 3, and 8. Class II contains six members, including HDACs 4, 5, 6, 7, 9 and 10 while class III HDACs, also known as Sirtuins, are NAD^+-dependent enzymes and have seven members (Sirt1-7).

***Corresponding authors:** Tel.: +84-4-39330531; Fax: +84-4-39332332; Emails: namnh@hup.edu.vn (N.H. Nam & P.T.P. Dung); shan@chungbuk.ac.kr (S.B. Han)

Lastly, class IV has only one member (HDAC11) and displays properties of both class I and class II HDACs.[4]

It has been widely demonstrated that inhibition of HDACs results in cell differentiation, apoptosis and cell-cycle arrest in a number of cancer cell lines. The effects have also been demonstrated in *in vivo* preclinical models.[5-12] HDAC inhibitors have, therefore, become a promising class of anticancer agents.[8-11] Extensive effort over the past decades has resulted in the identification of many potent HDAC inhibitors, including SAHA (suberoylanilide hydroxamic acid, Vorinostat), PXD-01 (Belinostat), LBH-589 (Panobinostat), MS-27-527 (Entinostat), and romidepsin (Figure 1).[13-15] Of these, two inhibitors including SAHA (trade name, Zolinza®) and romidepsin (tradename, Istodax®) have been approved by the FDA in 2006 and 2009, respectively, to treat cutaneous T-cell lymphoma.

As part of our research program to further explore novel hydroxamic acids as potential inhibitors of HDACs and anticancer agents, we have directed our efforts on heterocyclic analogues of SAHA. Previously, we have reported a series of benzothiazole-based hydroxamic acids with very potent HDAC inhibitory activity as well as cytotoxicity (Figure 2).[16] From this series, N^1-(6-chlorobenzo[d]thiazol-2-yl)-N^8-hydroxyoctanediamide (HUP00752), which possessed the most potent HDAC inhibition and cytotoxicity, was selected for further *in vivo* evaluation. It was shown that in the PC-3 prostate

cancer cells xenografted mice model, this compound exhibited *in vivo* antitumor efficacy equipotent to SAHA.[17] Currently, HUP00752 is being further developed as a promising anticancer agent. Encouraged by this success, we expanded our research with a series of 5-substitutedphenyl/aryl-1,3,4-thiadiazole-based hydroxamic acids (Figure 2) which are also very potent as HDAC inhibitors, possessing strong cytotoxicity.[18] Additionally, we have also investigated a series of isatin-based hydroxamic acids and found these compounds exhibited potent HDAC inhibition as well as strong cytotoxicity against several human cancer cell lines.[19] In continuity of our research program, we have designed, synthesized and evaluated a novel series of 2-oxoindoline-based hydroxamic acids. The current paper reports the results of this study.

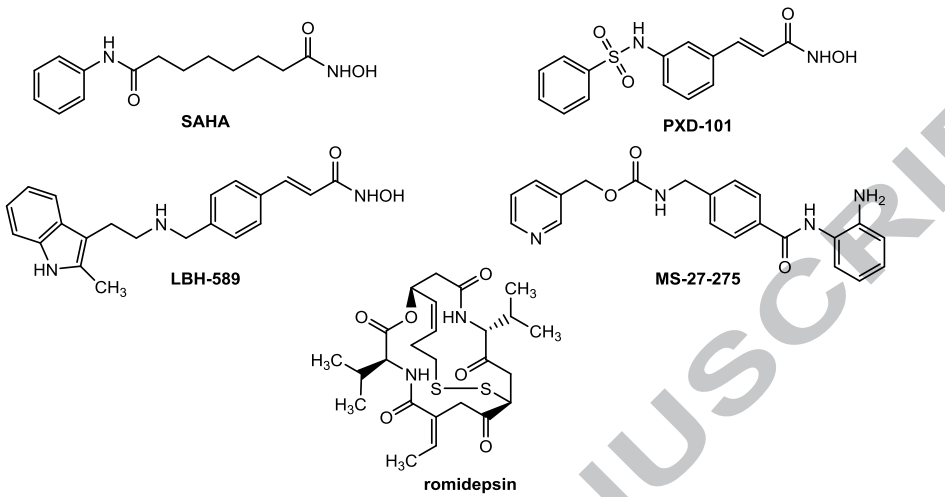

Figure 1. Structures of selected HDAC inhibitors

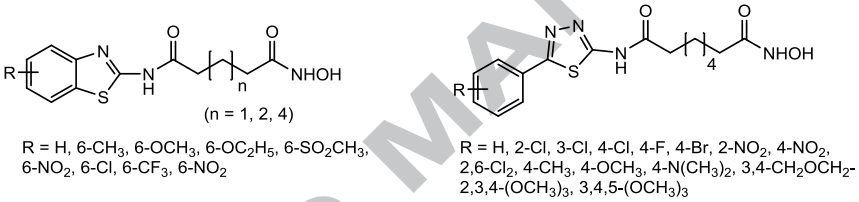

Figure 2. Structures of benzothiazole- and 5-substituted phenyl-1,3,4-thiadiazole-based hydroxamic acids

The synthesis of hydroxamic acids **3a-h** is illustrated in Scheme 1. In the first step, isatin and its 5- or 7-substituted derivatives were reacted with an excess of ethylene glycol in the presence of catalytic *p*-toluenesulfonic acid (*p*-TsOH) in refluxing dry toluene to give the dioxolane intermediates **2a-h**. Compounds **2a-h** were then reacted with ethyl 7-bromoheptanoate in DMF under alkaline conditions (K_2CO_3) with catalytic KI to furnish the heptanoates **3a-h** as brown-yellow oils in good overall yields (75-95%). Nucleophilic acyl substitution of heptanoates **3a-h** by hydroxylamine under basic conditions gave the final hydroxamic acids **4a-h** in good yields.

In a similar manner, two dithiolane compounds **7a** and **7f** were synthesized using ethylene dithiol instead of ethylene glycol (Scheme 1). The structures of the products were unambiguously determined using spectroscopic methods, including IR, MS, ^{1}H NMR and ^{13}C NMR, as well as elemental analysis (See ESI).

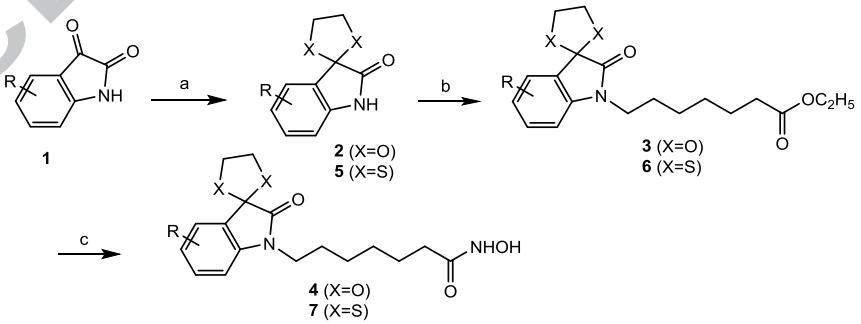

4 X = O

4a) R = H;	65%	
4b) R = 5'-F	69%	
4c) R = 5'-Cl	60%	
4d) R = 5'- Br	63%	
4e) R = 5'-NO_2	63%	
4f) R = 5'-CH_3	70%	
4g) R = 5'-OCH_3	70%	
4h) R = 7'-Cl	65%	

7 X= S

7a) R = H	65%
7f) R = 5'-CH_3	61%

Scheme 1. Synthesis of 2′-oxospiro[1,3]dioxolane/dithiolane-2,3′-indoline-based hydroxamic acids. Reagents and conditions: a) ethylene glycol/ethylene dithiol, *p*-TsOH, toluene, Δ, 24 h; b) ethyl 7-bromoheptanoate, K_2CO_3, KI, DMF, 60 ^{o}C, 24 h; c) hydroxylamine hydrochloride, NaOH, MeOH/THF, -5 ^{o}C, 30-60 min.

Because the compounds in this study were designed as analogues of SAHA, we expected them to be at least cytotoxic as SAHA. Therefore, all synthesized compounds were evaluated for their cytotoxicity. Initially the compounds were screened for cell growth inhibition against the SW620 (human colon cancer) cell line at a fixed concentration of 30 μM using the SRB method[20] with some modifications.[21,22] It was found that at this concentration, all ten compounds completely inhibited the growth of SW620 cells. The compounds, therefore, were further evaluated at 5 concentrations (e.g. 30, 10, 3, 1, 0.3 μM) with SW620 and two further human cancer cell lines, including PC-3 (prostate cancer) and AsPC-1 (pancreas cancer). The IC_{50} values of each compound were calculated[23] (Table 1). In this assay, SAHA was employed as a positive control. The data shown in Table 1 clearly indicated that most compounds in this series displayed potent cytotoxicity in all three human cancer cell lines tested, with IC_{50} values ranging from 0.05 to 2.90 μM. It was found that compound **4g** was the most potent with IC_{50} values of 0.05, 0.07 and 0.07 μM in the SW620, PC-3, and AsPC-1 cell lines, respectively. This compound was up to 74-fold more potent than SAHA in terms of cytotoxicity. The least cytotoxic compound in these series, **4a**, was still comparably potent (IC_{50}: 2.69, 2.90, 1.60 μM) to SAHA (IC_{50}: 3.70, 1.64, 2.24 μM) in the three cell lines tested. The introduction of substituents such as halogens (-F, -Cl, -Br), $-NO_2$, $-CH_3$, or OCH_3, either at position 5′ or 7′ on the indoline moiety, in all cases, resulted in enhancement of cytotoxicity. At least within the **4a-f** series, substitution at position 7′ (compound **4h**, IC_{50}, 0.07, 0.09, 0.09 μM) seemed to be more favorable than substitution at position 5′ (compound **4c**, IC_{50}: 1.04, 0.53, 0.49 μM). Using the current results, it was not possible to the electronic effect of the substituents on the compounds' cytotoxicity. The 2′-oxospiro[1,3]dithiolane-2,3′-indoline derivatives (**7a**, **7f**) showed better cytotoxicity than the two corresponding dioxolane compounds (**4a**, **4f**). These results suggest that a bulkier 1,3-dioxolane moiety at position 3′ of the indoline part was tolerated and favorable for the cytotoxicity of the compounds, despite the fact that compounds **7a** and **7f** showed much higher logP values (Table 1) compared to others (**4a-f**, SAHA).

Next, to clarify whether the compounds exhibited cytotoxicity through inhibition of HDAC in a manner similar to SAHA, the synthesized hydroxamic acids (**4a-h**, **7a, 7f**) were evaluated for inhibitory effect of histone-H3 and histone-H4 deacetylation at concentrations of 3 μM using the Western Blot assay. Since deacetylation of histone proteins is generally affected by HDACs, the inhibitory effects of the compounds against HDACs could be postulated through their ability to inhibit the level of histone deacetylation in cells. As shown in Figure 3, overall, it was found that the compounds exhibited significant inhibition of histone deacetylation in SW620 cells. The levels of acetyl-histones-H4 in cells treated with compounds **4a-h**, and **7a, 7f** had almost comparable intensity as that in cells treated with SAHA, suggesting these compounds were equally effective in the inhibition of histone-H4 deacetylation as SAHA. The levels of acetyl-histones-H3 in cells treated with compounds **4a, 4f** and **4g** also appeared to be similar to that in cells treated with SAHA. Meanwhile, in cells treated with **4b-e, 4h** and **7a, 7f**, the levels of acetyl-histones-H3 were somewhat less intense than that in cells treated with SAHA. Nevertheless, the above results showed a relatively good correlation between the inhibition of histones-H3 and H4 deacetylation and cytotoxicity. Since histones-H3 and H4 deacetylation is regulated principally by HDAC2 and HDAC3,[24] it is reasonable to extrapolate that these compounds exert HDAC inhibitory effects. To further confirm this, we performed an additional evaluation of the HDAC inhibitory effects of the compounds using purified HDAC2 enzymes. The results in Table 1 clearly demonstrate that all compounds exhibited comparable inhibitory effects to SAHA against HDAC2 enzymes with some compounds, e.g. **4b-e**, even showing 2- to 6-fold greater effect than SAHA in terms of HDAC2 activity inhibition. It was, however, difficult to correlate the HDAC2 inhibitory activity and cytotoxicity. Thus, the possibility that the compounds, especially compounds **4b-e, 4h** and **7a, 7f**, might exert cytotoxicity through inhibition of other HDAC subtypes, e.g. HDAC6 or HDAC8, should not be excluded. A more comprehensive evaluation of HDAC inhibitory effects of these compounds, therefore, needs to be further performed to deduce a complete correlation between HDAC inhibition and cytotoxicity.

Table 1: HDAC inhibition and cytotoxicity of the compounds synthesized against several cancer cell lines

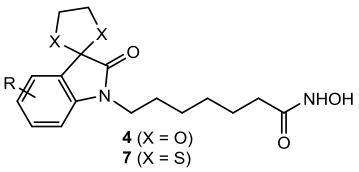

4 (X = O)
7 (X = S)

Comps	R	Molecular formula	Molecular weight	LogP[1]	HDAC2 inhibition (IC_{50},[2] μM)	Cytotoxicity (IC_{50},[2] μM)/Cell lines[3]		
						SW620	PC-3	AsPC-1
4a	-H	$C_{17}H_{22}N_2O_5$	334.37	1.15	0.16	2.68	2.90	1.60
4b	5′-F	$C_{17}H_{21}FN_2O_5$	352.36	1.35	0.06	1.48	1.86	1.01
4c	5′-Cl	$C_{17}H_{21}ClN_2O_5$	368.81	1.79	0.03	1.04	0.53	0.49
4d	5′-Br	$C_{17}H_{21}BrN_2O_5$	413.26	2.04	0.03	0.50	0.34	0.22
4e	5′-NO_2	$C_{17}H_{21}N_3O_7$	379.36	1.37	0.08	1.11	0.86	0.74
4f	5′-CH_3	$C_{18}H_{24}N_2O_5$	348.39	1.70	0.16	1.48	0.92	0.68
4g	5′-OCH_3	$C_{18}H_{24}N_2O_6$	364.39	1.23	0.12	0.05	0.07	0.07
4h	7′-Cl	$C_{17}H_{21}FN_2O_5$	352.36	1.79	0.15	0.07	0.09	0.09
7a	-H	$C_{17}H_{22}N_2O_3S_2$	366.50	3.95	0.32	0.84	0.89	0.86
7f	5′-CH_3	$C_{18}H_{24}N_2O_4S_2$	396.52	4.50	0.26	0.84	0.39	0.36

4			Tetrahedron				
SAHA[4]	264.32	1.44	0.20	1.44	0.053	2.24	

[1]Estimated by KOWWIN Software v1.67; [2]Concentration (μM) that produces a 50% reduction in cell growth or enzyme activity, the numbers represent the averaged results from triplicate experiments with deviation of less than 10%.; [3]Cell lines: SW620, colon cancer; PC-3, prostate cancer; AsPC-1, pancreatic cancer; [4]SAHA, suberoylanilide acid (positive control).

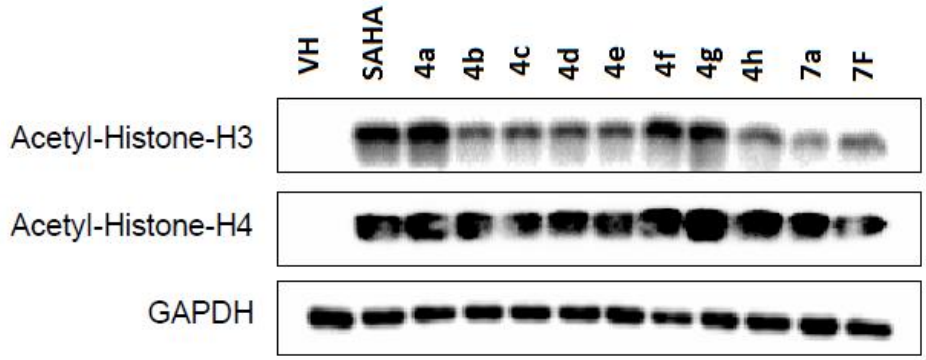

Figure 3. Effect on histone acetylation in SW620 cells. Cells were treated with compounds (3 μM) for 24 hrs. Levels of acetylated histone-H3 and -H4 in total cell lysates were determined by Western immunoblot analysis.

To gain insight into the main interaction between these compounds and HDAC, we performed docking experiments using the active site of HDAC. Since histone-H3 and histone-H4 deacetylation is principally regulated by HDAC2 and HDAC3[24] and the crystal structure of HDAC2 in complex with SAHA (PDB ID: 4LXZ) has been reported,[25] we decided to select the structure of HDAC2 in complex with SAHA as a docking template. In this study, we used AutoDock Vina[25] and executed control docking experiments with SAHA to the crystal structure of HDAC2 after SAHA was removed from the complex structures, as described previously.[16-19] It was found from docking experiments, that all of the compounds were located in the active site (Figure 4) of the enzyme and showed higher binding affinities (stabilization energy from -7.6 to -8.0 kcal/mol) than that of SAHA (stabilization energy, (-7.4 kcal/mol) (r.m.s.d distance from the original SAHA in the crystal structure : 0.609/2.056 Å). Overall, the binding affinities of individual compounds in both series **4** and **7** did not vary significantly in these docking studies. It seemed that changing the functional group at position 5′ or 7′ on the indoline moiety was not enough to affect calculation of the binding affinities using the program employed. On the binding mode, it was found that all compounds, except **4e** and **4h**, displayed very similar binding modes to that of compound **4a** (Figure 4). Compound **4e** was found to have a flipped orientation due to steric clash caused by the 5′-NO_2 functional group with Tyr209 and Leu276, meanwhile, the head group of compound **4h** was found to be rotated outward compared to compound **4a**, probably due to the presence of a chlorine substituent at position 7′ instead of position 5′ on the indoline system. The docking results indicate that within compound series **4** and **7**, changing the substituents has little effect on the binding affinities but are significantly influenced by the way the head group is orientated in the hydrophobic environment at the surface around the binding site of HDAC2.

In conclusion, we have reported a series of 2′-oxospiro[1,3]dioxolane-2,3′-indoline and two 2′-oxospiro[1,3]dithiolane-2,3′-indoline-based hydroxamic acids with potent cytotoxicity in tested human cancer cell lines and significant inhibitory effects against histone deacetylation in SW630 cells. From the results obtained it is clearly indicated that 2′-oxospiro[1,3]dioxolane-2,3′-indoline as well as 2′-oxospiro[1,3]dithiolane-2,3′-indoline systems can replace a phenyl ring as a cap group to create novel antitumor agents. Additionally, diverse substituents could be introduced at the 2′-oxospiro[1,3]dioxolane-2,3′-indoline moiety at both 5′ and 7′ positions, while still retaining bioactivity. These findings should encourage further exploration of the 2-oxoindoline moiety to produce more potent HDAC inhibitors with potential anticancer activity. Further evaluation of the inhibitory effects of these compounds against different HDAC subtypes and more in-depth docking studies are currently being carried out to delineate a quantitative correlation between the enzyme inhibition, enzyme affinities and their cytotoxicity.

Acknowledgements

We acknowledge the principal financial supports from the National Foundation for Science and Technology of Vietnam (NAFOSTED, Grant number 104.01-2013.16). The biological study was supported by the Medical Research Center program (MRC, Grant number 2010-0029480) and the docking study was supported by the Global Core Research Center (GCRC, Grant number NRF-2011-0030001**)** from the National Research Foundation (NRF) of Korea.

References

1. Nam, N. H.; Parang, K. *Curr. Drugs Targets* **2003**, *4*, 159-179.
2. Marks, P. A.; Rifkind, R.A.; Richon, V. M.; Breslow, R.; Miller, T.; Kelly, W. K. *Nature Rev. Cancer.* **2001**, *1*, 194-202.
3. Witt, O.; Deubzer, H. E.; Milde, T.; Oehme, I. *Cancer Lett*. **2009**, *277*, 8-21.
4. De Ruijter, A. J. M.; Gennip, A. H. V.; Caron, H. N.; Kemp, S.; Kuilenburg, A. B. P. V. *Biochem. J*. **2003**, *370*, 737-739.
5. Li, J.; Li, G.; Xu, W. *Curr Med. Chem*. **2013**, *20*, 1858-1886.
6. Ververis, K.; Hiong, A.; Karagiannis, T.C.; Licciardi, P. V. *Biologics* **2013**, *7*, 47-60.
7. Qiu, T.; Zhou, L.; Zhu, W.; Wang, T.; Wang, J.; Shu, Y.; Liu, P. *Future Oncol*. **2013**, *9*, 255-269.
8. West, A. C.; Johnstone, R. W. *J. Clin. Invest*. **2014**, *124*, 30-39.
9. Bolden, J. E.; Peart, M. J.; Johnstone, R.W. *Nat. Rev. Drug Discov*. **2006**, *5*, 769-784.
10. Dokmanovic, M.; Marks, P. A. *Expert Opin. Investi. Drug*. **2005**, *14*, 1497-1511.
11. Johnstone, R. W. *Nature Rev. Drug Disc.* **2002**, *1*, 287-299.
12. Glaser, K. B. *Biochem. Pharmacol.* **2007**, *74*, 659-871.
13. Dallavalle, S.; Cincinelli, R.; Nannei, R.; Merlini, L.; Morini, G.; Penco, S.; Pisano, C.; Vesci, L.; Barbarino, M.; Zuco, V.; De Cesare, M.; Zunino, F. *Eur J. Med. Chem.* **2009**, *44*, 1900-1912.

14. Bracker, T. U.; Sommer, A.; Fichtner, I.; Faus, H.; Haendler, B.; Hess-Stumpp, H. *Int. J. Oncol*. **2009**, *35*, 909-920.
15. Finnin, M. S.; Donigian, J. R.; Cohen, A.; Richon, V. M.; Rifkind, R. A.; Marks, P. A.; Breslow, R.; Pavietich, N. P. *Nature* **1999**, *401*, 188-193.
16. Oanh, D. T. K.; Hai, H. V.; Hue, V. T. M.; Park, S. H.; Kim, H. J.; Han, B. W.; Kim, H. S.; Hong, J. T.; Han, S. B.; Nam, N. H. *Bioorg. Med. Chem. Lett*. **2011**, *21*, 7509-7512.
17. Valente, S.; Mai, A. *Expert. Opin. Ther. Pat*. **2014**, *24*, 401-415.
18. Tung, T. T.; Oanh, D. T.; Dung, P. T.; Hue, V. T.; Park, S. H.; Han, B. W.; Kim, Y.; Hong, J. T.; Han, S. B.; Nam, N. H. *Med Chem*. **2013**, *9*, 1051-1057.
19. Nam, N. H.; Huong, T. L.; Dung, D. T. M.; Oanh, D. T. K.; Dung, P. T. P.; Kim, K. R.; Han, B. W.; Kim, Y. S.; Hong, J. T.; Han, S. B. *J. Enzyme Inhib. Med. Chem.* **2014**, (published online, doi:10.3109/14756366.2013.832238).
20. Nam, N. H.; Huong, T. L.; Dung, D. T. M.; Oanh, D. T. K.; Dung, P. T. P.; Quyen, D.; Kim, K. R.; Han, B. W.; Kim, Y. S.; Hong, J. T.; Han, S. B. *Eur. J. Med. Chem*. **2013**, *70*, 477-486.
21. Skehan, P.; Storeng, R.; Scudiero, D.; Monk, A.; MacMahon, J.; Vistica, D.; Warren, J. T.; Bokesch, H.; Kenney, S.; Boyd. M. R. *J. Natl. Cancer Inst.* **1990**, *82*, 1107-1112.
22. You, Y. J.; Kim, Y.; Nam, N. H.; Bang, S. C.; Ahn, B. Z. *Eur. J. Med. Chem.* **2004**, *39*, 189-193.
23. Kim, Y.; You, Y. J.; Nam, N. H. Ahn, B. Z. *Bioorg. Med. Chem. Lett.* **2002**, *12*, 3435-3438.
24. Wu, L.; Smythe, A. M.; Stinson, S. F.; Mullendore, L. A.; Monks, A.; Scudiero, D. A.; Paull, K D.; Koutsoukos, A. D.; Rubinstein, L. V.; Boyd, M. R.; Shoemaker, R. H. *Cancer Res*. **1992**, *52*, 3029-3034.
25. Pelzel, H. R.; Schlamp, C. L.; Nickells. *BMC Neuroscience* **2010**, *11*, 62 (http://www.biomedcentral.com/1471-2202/11/62).

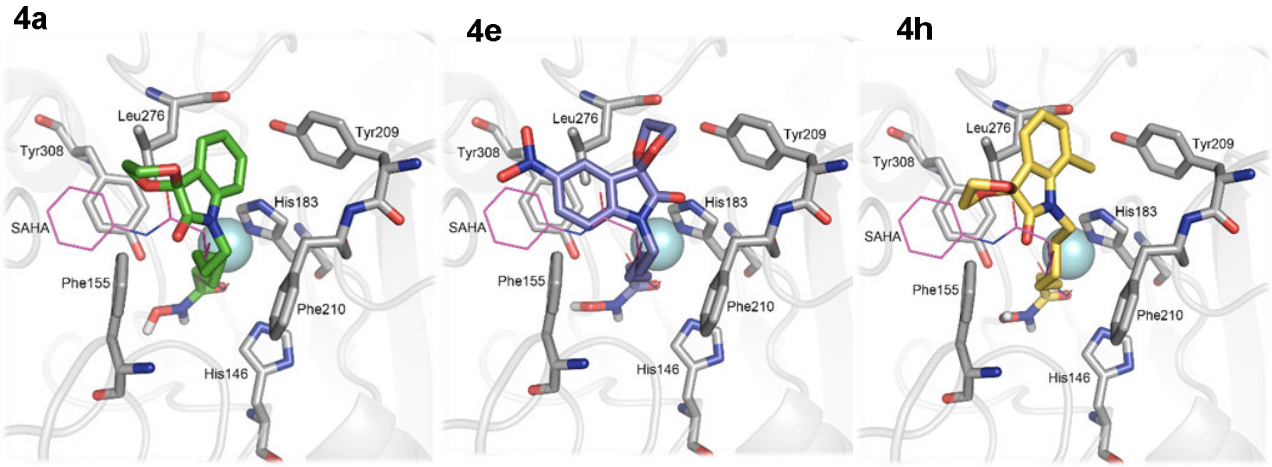

Figure 4. Stereoview of the actual binding pose of SAHA and simulated docking poses of compounds **4a**, **4e** and **4h** to HDAC2. SAHA is represented as a stick model in grey color. Compounds **4a**, **4e** and **4h** are shown as a stick model with carbon colored in bright green, blue and yellow; nitrogen, and oxygen atoms colored in dark blue and red, respectively. Important parts of the enzyme for interaction were shown as a stick model with carbon, nitrogen, and oxygen colored as grey, blue and red, respectively. Zn^{2+} ion is shown as a cyan sphere.